Performance Analysis of Uplink Massive MIMO System over Rician Fading Channel

Amare Kassaw*, Dereje Hailemariam†, A. M. Zoubir‡
*‡Signal Processing Group,TU-Darmstadt; *†Addis Ababa Institute of Technology, Addis Ababa University
Email: *akassaw@spg.tu-darmstadt.de, †derejeh.hailemariam@aait.edu.et,‡ zoubir@spg.tu-darmstadt.de

***Abstract*—Massive multiple input multiple output (MIMO) is considered as one of the promising technology to significantly improve the spectral efficiency of fifth generation (5G) networks. In this paper, we analyze the performance of uplink massive MIMO systems over a Rician fading channel and imperfect channel state information (CSI) at a base station (BS). Major Rician fading channel parameters including path-loss, shadowing and multipath fading are considered. Minimum mean square error (MMSE) based channel estimation is done at the BS. Assuming a zero-forcing (ZF) detector, a closed-form expression for the uplink achievable rate is derived and expressed as a function of system and propagation parameters. The impact of the system and propagation parameters on the achievable rate are investigated. Numerical results show that, when the Rician K-factor grows, the uplink achievable sum rate improves. Specifically, when both the number of BS antenna and the Rician K-factor become very large, channel estimation becomes more robust and the interference can be average out and thus, uplink sum rate improves significantly.**

***Index Terms*—Massive MIMO, Spectral Efficiency, Zero Forcing Detector.**

I. Introduction

Emergence of various mobile broadband services is causing a substantial increase in mobile data traffic [1]. In order to support this mobile data traffic, making the best use of unutilized spectrum and increasing spectral efficiency of the transmission systems are among the major recommendations of 5G mobile networks [1], [2]. 5G has to rely on technologies that can offer major increase in spectral efficiency [3]–[5]. By adopting very large number of antennas at the BS, which is called massive MIMO, 5G can significantly improve the spectral efficiency [2]. In addition, massive MIMO simplifies the transmission processing, improves the energy efficiency, and reduces the transmission power of each user [6], [7], [12]. Thus, it is expected to be an enabler for the deployment of future 5G mobile networks [1], [2].

Various studies have been conducted to analyze the spectral efficiency of massive MIMO systems [4]–[7], [9]. The studies show that when the number of antennas at the BS increases, massive MIMO systems can achieve large improvements in terms of spectral efficiency and link reliability [6], [7]. However, most of the previous research works on massive MIMO assume an independent and identically distributed (i.i.d) Rayleigh fading channel model, which does not take into account the line-of-sight (LOS) link that may be dominant in many realistic scenarios. While this assumption helped to simplify mathematical manipulations, it cannot capture the fading characteristics when there is LOS between the transmitter and receiver [13]. The previous works also assume the availability of perfect CSI at the BS. But, in real situations, the true channel matrix is unknown and should be estimated at the BS [7]. Furthermore, most works do not account for important propagation parameters such as path loss, shadowing and multipath fading. Thus, to understand all impacts of the wireless channel, more general fading models should be considered.

Thus, in this work, we evaluate the performance of massive MIMO systems over a Rician fading channel model. In this model, the multipath fading channel matrix consists of a deterministic LOS component and a random non-line-of-sight (NLOS) component [9], [13]. This model can represent the real propagation environment [15] and represent well several real scenarios such as indoor, vehicle-to-vehicle and millimeter wave (mmWave) communications [8], [14]. We consider a single-cell uplink massive MIMO and a zero forcing (ZF) detector. Further, we assume availability of imperfect CSI at the BS and thus, MMSE based channel estimation is done to determine the true channel matrix.

In this paper, we derive the estimate of the Rician fading channel and variance of the estimation error; formulate closed-form expression for the uplink achievable rate of massive MIMO with ZF detector in terms of system and propagation parameters. Further, the impacts of these parameters are analyzed and numerical simulations are done to validate theoretical analysis.

The rest of the paper is organized as follows. In Section II, the system and channel models for a single cell uplink massive MIMO are presented. In Section III, a closed-form expression of the achievable rate of the ZF detector with imperfect CSI is formulated. Numerical results are discussed in Section IV and conclusions are drawn in Section V.

II. The System and Channel Model

We consider a single cell uplink massive MIMO system model shown in Figure 1 where the BS is equipped with M antennas to serve N single-antenna users in the same time-frequency resource. If $\sqrt{\mathrm{p}_u}\,\mathbf{x}$ denotes the complex valued $N\times 1$ simultaneously transmitted signal vector by the N users, then the $M \times 1$ received signal vector $\mathbf{y}$ at the BS is [7]

$$\mathbf{y} = \sqrt{\mathrm{p}_u}\mathbf{G}\mathbf{x} + \mathbf{n} \tag{1}$$

ISBN 978-90-827970-1-5 © EURASIP 2018

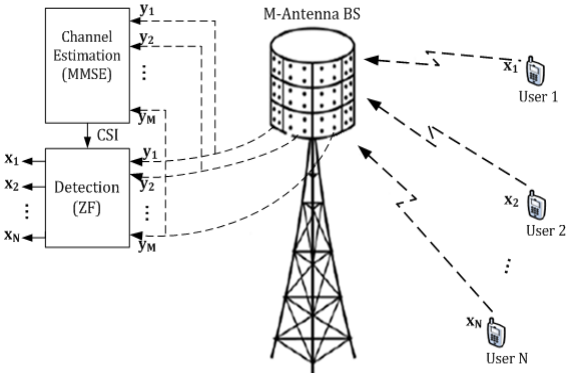

Fig. 1. Single-cell uplink massive MIMO system model.

where $\mathbf{G}$ represents an $M \times N$ Rician fading channel matrix between the BS and the N users with $\mathrm{g}_{mn} \triangleq [\mathbf{G}]_{mn}$ being the channel coefficient between the m^{th} antenna of the BS and the n^{th} user, p_u is the average transmitted power of each user and $\mathbf{n}$ is additive white Gaussian noise vector with zero mean and unit variance. From the received signal vector $\mathbf{y}$ together with knowledge of CSI, the BS detects the signals transmitted from N users [7]. To facilitate our analysis, we first define uplink Rician channel model.

A. Uplink Rician Fading Channel Model

In MIMO wireless systems, the physical channel between the user and the BS antennas is subjected to pathloss, shadowing and multipath fading effects. Considering all the propagation effects, the Rician fading massive MIMO channel model is formulated as [4]

$$\mathbf{G} = \mathbf{H}\mathbf{D}^{\frac{1}{2}} \tag{2}$$

where an $N \times N$ matrix $\mathbf{D} = \mathrm{diag}\{\beta_1, \beta_2, \cdots, \beta_N\}$ represents the large scale propagation matrix that includes pathloss and shadowing effects with elements $\beta_n = \mathrm{d}_n^{-\upsilon}\psi_n$, d_n is the Euclidean distance between the BS antenna and the n^{th} user, υ is the pathloss exponent, and ψ_n represents a log-normal shadowing with $10\log_{10}\psi_n \sim \mathcal{N}(0, \sigma_{\mathrm{sh}}^2)$ where σ_{sh} is the standard deviation of the shadow fading model [4].
The matrix $\mathbf{H} \in \mathcal{C}^{\mathrm{M}\times\mathrm{N}}$ represents the multipath fading effect. It can be modeled with the Rayleigh or Rician distribution [8].This is to use Rician fading channel model in our work. In this model, the matrix $\mathbf{H}$ consists of two parts; a deterministic component that represent the LOS signals and a Rayleigh-distributed random component which accounts for the NLOS signals. In this case, $\mathbf{H}$ is formulated as [8]

$$\mathbf{H} = \bar{\mathbf{H}}\left(\frac{\Omega}{\Omega + \mathbf{I}_N}\right)^{\frac{1}{2}} + \mathbf{H}_r\left(\frac{1}{\Omega + \mathbf{I}_N}\right)^{\frac{1}{2}} \tag{3}$$

where $\bar{\mathbf{H}}$ is an $M \times N$ matrix that represents the deterministic component in which $[\bar{\mathbf{H}}]_{mn} = e^{-j(m-1)\frac{2\pi\gamma}{\lambda}\sin(\theta_n)}$, when γ is the antenna spacing and λ is the wave length, θ_n is the arrival angle of the n^{th} user signal, Ω is an N × N diagonal matrix with $[\Omega]_{nn} = K_n$, K_n is the Rician factor of each user which shows the ratio of the power of the deterministic component to the power of the scattered components [8] and $\mathbf{H}_r$ denotes the random NLOS component, the entries of which are assumed to be i.i.d Gaussian random variables with zero-mean and unit variance. Finally, based on (3), Equation (2) is modified as

$$\mathbf{G} = \bar{\mathbf{G}}\left(\frac{\Omega}{\Omega + \mathbf{I}_N}\right)^{\frac{1}{2}} + \mathbf{G}_r\left(\frac{1}{\Omega + \mathbf{I}_N}\right)^{\frac{1}{2}} \tag{4}$$

where $\bar{\mathbf{G}}$ denotes the LOS component of $\mathbf{G}$ ($\bar{\mathbf{G}} = \bar{\mathbf{H}}\mathbf{D}^{\frac{1}{2}}$) and $\hat{\mathbf{G}}_r$ represents the random component of $\mathbf{G}$ ($\mathbf{G}_r = \mathbf{H}_r\mathbf{D}^{\frac{1}{2}}$). In this work, we assume $\mathbf{H}_r$ is unknown at the BS and pilot based channel estimation is done in Section II-B.

B. Uplink Channel Estimation

In real situations, the true channel matrix $\mathbf{G}$ is unknown and estimated at the BS. To simplify the analysis, we assume that both the LOS component and the Rician K-factor matrix Ω are perfectly known at both the BS and user. Thus, estimation is done only for the Rayleigh-distributed random component. In this assumption, the estimate of $\mathbf{G}$ can be expressed as [8]

$$\hat{\mathbf{G}} = \bar{\mathbf{G}}\left(\frac{\Omega}{\Omega + \mathbf{I}_N}\right)^{\frac{1}{2}} + \hat{\mathbf{G}}_r\left(\frac{1}{\Omega + \mathbf{I}_N}\right)^{\frac{1}{2}} \tag{5}$$

where $\hat{\mathbf{G}}_r$ represents the estimate of the random component of $\mathbf{G}$ ($\mathbf{G}_r = \mathbf{H}_r\mathbf{D}^{\frac{1}{2}}$). It is stated in [7] that the channel can be estimated using uplink pilots. Let T be the length (time-bandwidth product) of the coherence interval and let $\tau(\tau \leq T)$ be the number of symbols used for uplink training. In the training stage, all users simultaneously transmit the pilot sequences of τ-symbols. The pilot sequences of the N users can be represented by a $\tau \times N$ matrix $\sqrt{p_p}\mathbf{\Phi}$ and we assume $\mathbf{Z}^{\mathrm{H}}\mathbf{Z} = \mathbf{I}_N$ where $\mathbf{Z} \triangleq \mathbf{\Phi}[(\Omega + \mathbf{I}_N)^{-1}]^{\frac{1}{2}}$, and $p_{_p} = \tau p_u$ is the transmit pilot power. Then, the $M \times \tau$ received pilot matrix at the BS is given by [8]

$$\mathbf{Y}_{\mathrm{p}} = \sqrt{p_{_{\mathrm{p}}}}\mathbf{G}\mathbf{\Phi}^T + \boldsymbol{\mathcal{N}} \tag{6}$$

where $\boldsymbol{\mathcal{N}}$ is an $M \times \tau$ matrix with i.i.d $\mathcal{CN}(0,1)$ elements. Removing the LOS component from $\mathbf{G}$ in (4), which is assumed to be known a-priori, and substituting the remaining terms into (6), the received pilot matrix becomes

$$\mathbf{Y}_{\mathrm{p},\,r} = \sqrt{p_p}\mathbf{G}_r\left(\frac{\Omega}{\Omega + \mathbf{I}_N}\right)^{\frac{1}{2}}\mathbf{\Phi}^T + \boldsymbol{\mathcal{N}} \tag{7}$$

which can be simplified further as

$$\mathbf{Y}_{\mathrm{p},\,r} = \sqrt{p_p}\mathbf{G}_r\mathbf{Z}^T + \boldsymbol{\mathcal{N}}. \tag{8}$$

Channel estimation is done to estimate $\mathbf{G}_r$ from $\mathbf{Y}_{\mathrm{p},\,r}$. For this, we derive the MMSE based channel estimation [16] and summarize the result in Theorem 2.1.

Theorem 2.1: Given a $\tau \times N$ transmitted pilot matrix $\sqrt{p_p}\mathbf{\Phi}$ which satisfies $\mathbf{Z}^{\mathrm{H}}\mathbf{Z} = \mathbf{I}_N$ where $\mathbf{Z} \triangleq \mathbf{\Phi}[(\Omega + \mathbf{I}_N)^{-1}]^{\frac{1}{2}}$ and $p_{_p} = \tau p_u$ is the transmit pilot power, the MMSE based estimate of the random component of the Rician fading channel, $\hat{\mathbf{G}}_r$, obtained from the received pilot matrix $\mathbf{Y}_{\mathrm{p},\,r}$ is

$$\hat{\mathbf{G}}_r = \frac{1}{\sqrt{p_p}}\mathbf{Y}_{p,r}\mathbf{Z}^*\tilde{\mathbf{D}} = \left(\mathbf{G}_r + \frac{1}{\sqrt{p_p}}\mathbf{W}\right)\tilde{\mathbf{D}} \tag{9}$$

ISBN 978-90-827970-1-5 © EURASIP 2018

where $\tilde{\mathbf{D}} \triangleq (\frac{1}{p_p}\mathbf{D}^{-1} + \mathbf{I}_N)^{-1}$ and $\mathbf{W} \triangleq \boldsymbol{\mathcal{N}}\boldsymbol{Z}^*$. With $\mathbf{Z}^H\mathbf{Z} = \mathbf{I}_N$, the entries of $\mathbf{W}$ are i.i.d $\mathcal{CN}(0,1)$. *The proof is shown in Appendix I.*

III. Achievable Rate of the ZF Detector with Imperfect CSI

In this Section, we derive an expression of the uplink achievable rate of massive MIMO with a ZF detector and imperfect CSI assumption at the BS. For this, we first formulate the general expression of the uplink achievable rate with linear detection as follows. Let $\mathcal{E} \triangleq \hat{\mathbf{G}} - \mathbf{G}$ denotes the error incurred due to channel estimation and let an $M \times N$ matrix $\hat{\mathbf{A}}$ be the model for the linear detector which depends on $\hat{\mathbf{G}}$ and $\mathcal{E}$, then the BS processes the received symbol vector by multiplying it with $\hat{\mathbf{A}}^{\mathrm{H}}$. Thus, we get [7]

$$\hat{\mathbf{r}} = \hat{\mathbf{A}}^{\mathrm{H}}\mathbf{y} = \sqrt{p_u}\hat{\mathbf{A}}^{\mathrm{H}}(\hat{\mathbf{G}}\mathbf{x} - \mathcal{E}\mathbf{x}) + \hat{\mathbf{A}}^{\mathrm{H}}\mathbf{n}. \tag{10}$$

where $\mathbf{y}$ is the received signal vector given in 1. Based on (10), the received signal for the n^{th} user is given by (11) where $\hat{\mathbf{a}}_n$ is the n^{th} column of $\hat{\mathbf{A}}$, and $\hat{\mathbf{g}}_i$ and $\mathcal{E}_i$ are the i^{th} columns of $\hat{\mathbf{G}}$ and $\mathcal{E}$, respectively. The last three terms in (11) correspond to intra-cell interference, channel estimation error and noise respectively. Owing to the properties of MMSE estimation [16], the channel estimation error is uncorrelated with both the channel estimate and the received pilot signal. In this case, the variance of the elements of the channel estimation error, $\mathcal{E}_i$ is [8]

$$\mathbb{E}\{|[\mathcal{E}]_{mi} - \mathbb{E}\{[\mathcal{E}]_{mi}\}|^2\} = \frac{\beta_i}{(1 + p_{\mathrm{p}}\beta_i)(K_i + 1)} \tag{12}$$

where $m = 1, 2, \cdots, M$ and $i = 1, 2, \cdots, N$. The BS treats the channel estimate as the true channel and the part including the last three terms of (11) is considered as interference and noise [4]. Thus, the uplink achievable rate of the n^{th} user with linear detector is given by (13). And the uplink achievable sum rate per cell is given by [4]

$$\mathrm{R}_s = \frac{T - \tau}{T}\sum_{n=1}^{N} R_n. \tag{14}$$

From the general formulation in (13), we derive the uplink achievable rate of the ZF detector as follows. For a ZF detector with imperfect CSI at the BS, the detection matrix is given by $\hat{\mathbf{A}} = \hat{\mathbf{G}}(\hat{\mathbf{G}}^{\mathrm{H}}\hat{\mathbf{G}})^{-1}$. For $M > N$, $\hat{\mathbf{A}}^{\mathrm{H}}\hat{\mathbf{G}} = \mathbf{I}_N$ and thus, $\hat{\mathbf{a}}_n^H\hat{\mathbf{g}}_i = 1$ if $n = i$ and zero otherwise [4]. Based on this assumption, and by using (12) and (13), the achievable rate of the ZF detector is given by

$$\mathrm{R}_n^{\mathrm{ZF}} = \mathbb{E}\Big\{\log_2\big(1 + \frac{p_u}{(\sum_{i=1}^{N}\frac{p_u\beta_i}{(1+p_p\beta_i)(K_i+1)} + 1)[(\hat{\mathbf{G}}^{\mathrm{H}}\hat{\mathbf{G}})^{-1}]_{\mathrm{nn}}}\big)\Big\}. \tag{15}$$

From (15), we can see that when the Rician K-factor becomes large, the summation term decreases and thus, the uplink achievable rate increases. But, (15) incorporates a non-central Wishart distribution which is cumbersome to evaluate. Thus, by calculating the approximate moments of the non-central Wishart distribution, we drive a closed-form expression for the achievable rate in (15). To this end, a closed-form expression for the achievable rate is formulated as a function of system and propagation parameters.

A. Closed-form Expression of the Achievable Rate of a ZF Detector

Theorem 3.1 formulates a closed-form expression of the uplink achievable rate of the n^{th} user with a ZF detector in (15). It is formulated as a function of BS antenna, number of users, large scale fading parameter and the Rician K-factor.

Theorem 3.1: The achievable rate of the n^{th} user with a ZF detector and imperfect CSI at the BS can be approximated by

$$\mathrm{R}_n^{\mathrm{ZF}} = \log_2\left(1 + \frac{p_u\beta_n(M-N)}{(\sum_{i=1}^{N}\frac{p_u\beta_i}{(1+p_p\beta_i)(K_i+1)} + 1)[\hat{\boldsymbol{\Sigma}}^{-1}]_{\mathrm{nn}}}\right) \tag{16}$$

where

$$\begin{aligned}\hat{\boldsymbol{\Sigma}} &= \boldsymbol{\Sigma} + \frac{1}{M}[\Omega(\Omega + \mathbf{I}_N)^{-1}]^{\frac{1}{2}}\bar{\mathbf{H}}^{\mathrm{H}}\bar{\mathbf{H}}[\Omega(\Omega + \mathbf{I}_N)^{-1}]^{\frac{1}{2}} \\ \boldsymbol{\Sigma} &= \mathrm{diag}\{\frac{\eta_n}{K_n + 1}\} \qquad \text{for } n = 1, 2, \cdots, N.\end{aligned} \tag{17}$$

Proof: Starting from (15), noting the convexity of $\log(1 + \frac{1}{x})$, and applying Jensen's inequality [4], we get

$$\mathrm{R}_n^{\mathrm{ZF}} = \log_2\left(1 + \frac{p_u\beta_n}{(\sum_{i=1}^{N}\frac{p_u\beta_i}{(1+p_p\beta_i)(K_i+1)} + 1)\mathbb{E}\{[(\hat{\mathbf{H}}^{\mathrm{H}}\hat{\mathbf{H}})^{-1}]_{\mathrm{nn}}\}}\right) \tag{18}$$

where $\hat{\mathbf{H}}$ is the multipath fading part of the estimated channel matrix in (5) and is given by

$$\hat{\mathbf{H}} = \bar{\mathbf{H}}[\Omega(\Omega + \mathbf{I}_N)^{-1}]^{\frac{1}{2}} + (\hat{\mathbf{H}}_r + \frac{1}{\sqrt{p_p\beta_n}}\mathbf{W})\tilde{\mathbf{D}}[(\Omega + \mathbf{I}_N)^{-1}]^{\frac{1}{2}}. \tag{19}$$

When $\hat{\mathbf{H}}$ follows a normal distribution with non-zero mean, $\mathbf{W} \triangleq \hat{\mathbf{H}}^{\mathrm{H}}\hat{\mathbf{H}}$ follows a non-central Wishart distribution denoted by $\mathbf{W} \sim \mathcal{W}_N(M, \mathbf{P}, \boldsymbol{\Sigma})$, where $\mathbf{P}$ is the mean matrix of $\hat{\mathbf{H}}$ and $\boldsymbol{\Sigma}$ is the covariance matrix of the row vectors of $\hat{\mathbf{H}}$ [9] with values $\mathbf{P} = \bar{\mathbf{H}}[\Omega(\Omega + \mathbf{I}_N)^{-1}]^{\frac{1}{2}}$ and $\boldsymbol{\Sigma} = (\Omega + \mathbf{I}_N)^{-1}\eta_n$ with $\eta_n = \frac{p_p\beta_n}{1+p_p\beta_n}$. It is quite complicated and cumbersome to analyze this non-central Wishart distribution directly. In this case, to simplify the analysis, the non-central Wishart distribution has been approximated by a central Wishart distribution as [9]

$$\hat{\mathbf{W}} \sim \mathcal{W}_N(M, \hat{\boldsymbol{\Sigma}}) \tag{20}$$

where $\hat{\boldsymbol{\Sigma}} = \boldsymbol{\Sigma} + \frac{1}{M}\mathbf{P}^H\mathbf{P}$. Now, let $\mathbf{r}_n = \frac{1}{[(\hat{\mathbf{H}}^{\mathrm{H}}\hat{\mathbf{H}})^{-1}]_{\mathrm{nn}}}$. With the above approximation, $\mathbf{r}_n$ is a Chi-square random variable [9]. Based on this fact, we proved in Appendix II that the first moment of the inverse Wishart distribution is expressed as

$$\mathbb{E}\{[(\hat{\mathbf{H}}^{\mathrm{H}}\hat{\mathbf{H}})^{-1}]_{\mathrm{nn}}\} = \frac{[\hat{\boldsymbol{\Sigma}}^{-1}]_{\mathrm{nn}}}{\mathrm{M\text{-}N}}. \tag{21}$$

Finally, substituting (21) into (18), we get (16).

We performed numerical simulations to compare (16) with (15) and to analyze the effects of the system and propagation parameters. As it is shown in (16), the achievable rate increases

ISBN 978-90-827970-1-5 © EURASIP 2018

$$\hat{r}_n = \sqrt{p_u}\hat{\mathbf{a}}_n^{\mathrm{H}}\hat{\mathbf{g}}_n x_n + \sqrt{p_u}\sum_{i=1,i\neq n}^{N}\hat{\mathbf{a}}_n^{\mathrm{H}}\hat{\mathbf{g}}_i x_i - \sqrt{p_u}\sum_{i=1}^{N}\hat{\mathbf{a}}_n^{H}\mathcal{E}_i x_i + \hat{\mathbf{a}}_n^{H}\mathbf{n}. \tag{11}$$

$$\mathrm{R}_n = \mathbb{E}\left\{\log_2\left(1+\frac{\mathrm{p}_u|\hat{\mathbf{a}}_n^{\mathrm{H}}\hat{\mathbf{g}}_n|^2}{\mathrm{p}_u\sum_{i=1,\,i\neq n}^{N}|\hat{\mathbf{a}}_n^{\mathrm{H}}\hat{\mathbf{g}}_i|^2+\sum_{i=1}^{N}\|\hat{\mathbf{a}}_n\|^2\frac{p_u\beta_i}{(1+p_p\beta_i)(K_i+1)}+\|\hat{\mathbf{a}}_n\|^2}\right)\right\}. \tag{13}$$

when the number of BS antennas grows large. Besides, when the Rician K-factor becomes large, the interference term vanishes and thus the achievable rate increases.

B. Achievable Rate at a Large Rician K-factor

At a large Rician K-factor, that is when $K_n \to \infty$, the summation term in (16) and $\mathbf{\Sigma}$ in (17) goes to zero. Thus, the achievable rate in (17) converges to

$$\mathrm{R}_n^{\mathrm{ZF}} = \log_2\left(1+\frac{p_u\beta_n(M-N)}{[\hat{\mathbf{\Sigma}}^{-1}]_{\mathrm{nn}}}\right) = \log_2\left(1+\frac{p_u\beta_n(M-N)}{[(\frac{1}{M}\bar{\mathbf{H}}^{\mathrm{H}}\bar{\mathbf{H}})^{-1}]_{\mathrm{nn}}}\right). \tag{22}$$

The achievable rate in (22) is the same as the achievable rate with a perfect CSI in [12]. This shows that when the Rician K-factor grows without bound, the approximation of the achievable rate converges to the same value regardless of the CSI quality [12]. Further, when M grows large, $\frac{1}{M}\bar{\mathbf{H}}^{\mathrm{H}}\bar{\mathbf{H}}$ becomes asymptotically an identity matrix [12], [14]. In this case, Equation (22) converges to

$$\mathrm{R}_n^{\mathrm{ZF}} = \log_2\left(1+p_u\beta_n(M-N)\right). \tag{23}$$

This shows that when both the Rician K-factor and the BS antenna become very large, the effects of small scale fading is completely averaged out and intra-cell interference disappears completely [8]. Thus, the uplink achievable rate will only depend on the number of BS antenna and large scale fading parameters.

IV. Numerical Results and Analysis

We consider a single cell uplink massive MIMO system with cell radius of $r_{\mathrm{c}} = 1000$ meters. The N users are distributed uniformly over the cell except for an exclusion zone around the BS ($r_{\mathrm{h}} \leq 100$ meter). The exclusion zone is assumed to ensure that uplink and downlink communication happens in the far field of the transmitting antenna and plane waves can be assumed at the receiver [4]. The large scale fading is modeled as $\beta_n = z_n(\frac{r_n}{r_{\mathrm{h}}})^{-v}$ where z_n is the log-normal shadow fading random variable with standard deviation $\sigma_{\mathrm{sh}} = 8$dB, $v = 3.8$ is the path loss exponent, and $r_n \in [r_{\mathrm{c}}, r_{\mathrm{h}}]$ denotes the distance between the n^{th} user and the BS [4]. To simplify the analysis, we assume that all users have similar Rician K-factors. The parameters of modulated data streams are chosen according to the LTE standard [4] with a symbol interval $T_s = 71.4\mu s$, a useful symbol duration $T_u = 66.7\mu s$, a channel coherence time $T_c = 1ms$ and thus a symbol time of the channel $T = \frac{T_c}{Ts}\frac{T_u}{T_s - T_u} = 196$ symbols and $\tau = N$.

We first analyze the impacts of the LOS component on the achievable rate. Figure 2 shows the uplink achievable sum rate of a Rician fading channel for different Rician K-factors. When the Rician K-factor increases, channel estimation becomes more robust and the effects of the random component of the Rician fading channel will be decreased and thus, the uplink achievable sum rate increases.

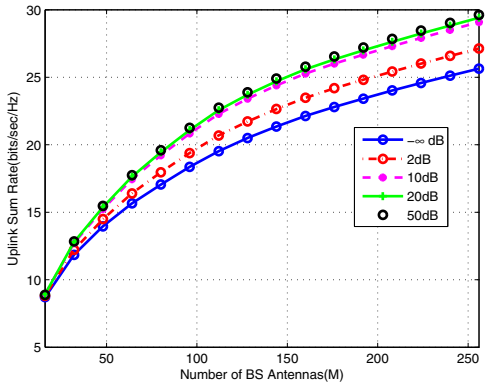

Fig. 2. Uplink sum rate of massive MIMO in a Rician fading channel model with a ZF detector and imperfect CSI. The number of users is $N = 10$, the transmit power per user is $p_u = 10dB$, the pilot symbol length is $\tau = 10$ and dB means decibel.

In Figure 3, we validate the feasibility and realization of Theorem 3.1. For this, we compare the simulated sum rates in (15) with the analytical approximations in (16) and (22) at different values of the Rician K-factor. As shown in the Figure, the analytical approximations are fitted with the simulated results. This shows that the proposed approximation for the non-central Wishart distribution is very accurate and physically valid. Specifically, for both very large M and Rician K-factor, channel estimation error decreases, the interference can be average out completely, and thus, the approximation of the achievable sum rate converges to the same value independent of the CSI quality.

V. Conclusion

In this work, we studied the performance of a massive MIMO system over a Rician fading channel. Considering imperfect CSI at the BS, MMSE based channel estimation is done. The uplink achievable rate of the user with a ZF detector is formulated. Further, by approximating the non-central Wishart distribution with a central Wishart distribution, a closed-form expression is derived for the uplink achievable rate. From theoretical and numerical analysis, we observed that when both the Rician K-factor and the number of BS antenna become very large, channel estimation becomes

ISBN 978-90-827970-1-5 © EURASIP 2018

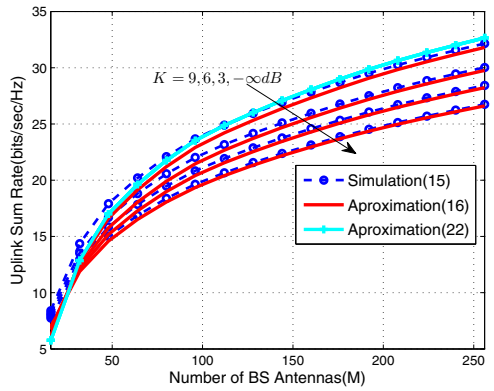

Fig. 3. Comparison of approximated and simulated results of uplink sum rate of massive MIMO in a Rician fading channel model with a ZF detector and imperfect CSI. The number of users is $N = 10$, the transmit power per user is $p_u = 10dB$, the pilot symbol length is $\tau = 10$.

more robust, the effect of small scale fading is averaged out and intra-cell interference disappears. Hence, the uplink achievable sum rate increases. This shows that massive MIMO systems are more suitable to be deployed in a Rician fading environment, especially when the LOS component is strong.

Appendix I : Proof of Theorem 2.1.

To find the MMSE based estimation of the Rician channel in (5) from (8), first dispread the received matrix in (8) by right multiplying with $(\mathbf{Z}^T)^H = \mathbf{Z}^*$ as

$$\mathbf{Y}' = \mathbf{Y}_{\mathrm{p},r}\mathbf{Z}^* = \sqrt{p_p}\mathbf{G}_r + \boldsymbol{\mathcal{N}}\mathbf{Z}^*. \tag{24}$$

Then, apply the MMSE estimator [16] on $\mathbf{Y}'$ to get $\hat{\mathbf{G}}_r$ as

$$\hat{\mathbf{G}}_r = \mathbb{E}\{\mathbf{G}_r|\mathbf{Y}'\} = \frac{\mathbf{C}_{\mathbf{G}_r\mathbf{Y}'}}{\mathbf{C}_{\mathbf{Y}'\mathbf{Y}'}}(\mathbf{Y}' - \mathbb{E}\{\mathbf{Y}'\}) + \mathbb{E}\{\mathbf{G}_r\} \tag{25}$$

where $\mathbf{C}_{\mathbf{G}_r\mathbf{Y}'}$ and $\mathbf{C}_{\mathbf{Y}'\mathbf{Y}'}$ are the covariance matrices. Noting that $\mathbb{E}\{\mathbf{Y}'\}$ and $\mathbb{E}\{\mathbf{G}_r\}$ are zero. The covariance matrices $\mathbf{C}_{\mathbf{Y}'\mathbf{Y}'}$ and $\mathbf{C}_{\mathbf{G}_r\mathbf{Y}'}$ are calculated as [16]

$$\begin{aligned}\mathbf{C}_{\mathbf{Y}'\mathbf{Y}'} &= \mathbb{E}\{\mathbf{Y}'(\mathbf{Y}')^H\} = p_p\mathbf{D} + \mathbf{I}_N \\ \mathbf{C}_{\mathbf{G}_r\mathbf{Y}'} &= \mathbb{E}\{\mathbf{G}_r(\mathbf{Y}')^H\} = \sqrt{p_p}\,\mathbf{D}.\end{aligned} \tag{26}$$

Substituting (26) into (25), we get

$$\begin{aligned}\hat{\mathbf{G}}_r &= \frac{\sqrt{p_p}\,\mathbf{D}}{p_p\mathbf{D} + \mathbf{I}_N}[\mathbf{Y}'] = \frac{\sqrt{p_p}\,\mathbf{D}}{p_p\mathbf{D} + \mathbf{I}_N}\mathbf{Y}_{\mathrm{p},r}\mathbf{Z}^* = \frac{1}{\sqrt{p_p}}\mathbf{Y}_{\mathrm{p},r}\mathbf{Z}^*\tilde{\mathbf{D}} \\ &= \left(\mathbf{G}_r + \frac{1}{\sqrt{p_p}}\mathbf{W}\right)\tilde{\mathbf{D}}.\end{aligned} \tag{27}$$

Appendix II: Proof of Equation (21).

For $\hat{\mathbf{W}} \sim \mathcal{W}_N(M, \hat{\boldsymbol{\Sigma}})$, $\mathbf{r}_n = \frac{1}{[(\hat{\mathbf{H}}^{\mathrm{H}}\hat{\mathbf{H}})^{-1}]_{\mathrm{nn}}}$ is a Chi-square random variable [9] with pdf given by [11]

$$f(\gamma_n) = \frac{[\hat{\boldsymbol{\Sigma}}^{-1}]_{\mathrm{nn}}}{\Gamma(M-N+1)}\exp\{-\gamma_n[\hat{\boldsymbol{\Sigma}}^{-1}]_{\mathrm{nn}}\}\Big(-\gamma_n[\hat{\boldsymbol{\Sigma}}^{-1}]_{\mathrm{nn}}\Big)^{\mathrm{M\text{-}N}} \tag{28}$$

To calculate the moment of the inverse Wishart distribution, $\mathbb{E}\{[(\hat{\mathbf{H}}^{\mathrm{H}}\hat{\mathbf{H}})^{-1}]_{\mathrm{nn}}\}$, let us express the integral $\int_0^\infty \frac{1}{\gamma_n}f(\gamma_n)\mathrm{d}\gamma_n$ as

$$\int_0^\infty \frac{1}{\gamma_n}f(\gamma_n)d\gamma_n = \frac{\mathrm{a}}{\mathrm{c}}\int_0^\infty \frac{e^{-\mathrm{a}x}(\mathrm{a}x)^d}{x}dx \tag{29}$$

where $x = \gamma_n$, $\mathrm{a} = [\hat{\boldsymbol{\Sigma}}^{-1}]_{\mathrm{nn}}$, $\mathrm{c} = \Gamma(M-N+1)$, and $\mathrm{d} = M-N$. Let $y = \mathrm{a}x$, then $dy = \mathrm{a}dx$. Substitute y and dy/a in place of x and dx we get

$$\begin{aligned}\frac{\mathrm{a}}{\mathrm{c}}\int_0^\infty \frac{e^{-ax}(ax)^d}{x}dx &= \frac{\mathrm{a}}{\mathrm{c}}\int_0^\infty e^{-y}y^{d-1}dy = \frac{\mathrm{a}}{\mathrm{c}}\Gamma(d) \\ &= [\hat{\boldsymbol{\Sigma}}^{-1}]_{\mathrm{nn}}\frac{\Gamma(M-N)}{\Gamma(M-N+1)} = \frac{[\hat{\boldsymbol{\Sigma}}^{-1}]_{\mathrm{nn}}}{M-N}\end{aligned} \tag{30}$$

Where $\Gamma(M) = (M-1)!$ is the Gamma function [11] and $\int_0^\infty e^{-1}t^{z-1}dt = \Gamma(z)$ for $z \in \mathbb{R}$. Hence, (30) concludes the proof and thus,

$$\mathbb{E}\{[(\hat{\mathbf{H}}^{\mathrm{H}}\hat{\mathbf{H}})^{-1}]_{\mathrm{nn}}\} = \frac{[\hat{\boldsymbol{\Sigma}}^{-1}]_{\mathrm{nn}}}{M-N}. \tag{31}$$

REFERENCES

[1] E. G. Larsson and O. Edfors and F. Tufvesson and T. L. Marzetta, "Massive MIMO for next generation wireless systems," *IEEE Communications Magazine*, vol. 52, pp. 186195, February 2014

[2] L. Lu and G. Y. Li and A. L. Swindlehurst and A. Ashikhmin and R. Zhang, "An overview of massive MIMO: benefits and challenges," *IEEE Journal of Selected Topics in Signal Processing*,vol. 8, pp. 742758, Oct 2014.

[3] F. Rusek, D. Persson, B. K. Lau, E. G. Larsson, T. L. Marzetta, O. Edfors, and F. Tufvesson, "Scaling up MIMO: Opportunities and challenges with very large arrays, ", *IEEE Signal Processing Magazine*,vol. 30, no. 1, pp. 4060, 2013.

[4] T. L. Marzetta, E. G. Larsson, H. Yang, and H. Q. Ngo, *Fundamentals of Massive MIMO*.Cambridge University Press, 2016.

[5] T. L. Marzetta, "Noncooperative cellular wireless with unlimited numbers of base station antennas, *IEEE Transactions on Wireless Communications,* vol. 9, no. 11, pp. 35903600, 2010.

[6] J. Hoydis, S. Ten Brink, and M. Debbah, "Massive MIMO in the UL/DL of cellular networks: How many antennas do we need?," *IEEE Journal on selected Areas in Communications*, vol. 31, no. 2, pp. 160171, 2013.

[7] H. Q. Ngo, E. G. Larsson, and T. L. Marzetta, "Energy and spectral efficiency of very large multiuser MIMO systems, *IEEE Transactions on Communications*, vol. 61, no. 4, pp. 14361449, 2013.

[8] D. W. Yue and G. Y. Li, "LOS-based conjugate beamforming and power-scaling law in massive MIMO systems," *arXiv preprint arXiv:1707.059*, 15, 07 2014.

[9] C. Siriteanu, Y. Miyanaga, and et al., "MIMO Zero-Forcing detection analysis for correlated and estimated Rician fading," *IEEE transactions on Vehicular Technology*, vol. 61, no. 7, pp. 30873099, 2012.

[10] J. Zhang, L. Dai, Z. He, S. Jin, and X. Li, "Performance analysis of mixed-ADC massive MIMO systems over Rician fading channels," *IEEE Journal on Selected Areas in Communications*, vol. 35, no. 6, pp. 1327 1338, 2017.

[11] D. K. Nagar and A. K. Gupta, "Expectations of functions of complex Wishart matrix," *Acta applicandae mathematicae*, vol. 113, no. 3, pp. 265288, 2011.

[12] Q. Zhang, S. Jin, K. K. Wong, H. Zhu, and M. Matthaiou, "Power scaling of uplink massive MIMO systems with arbitrary-rank channel means," *IEEE Journal of Selected Topics in Signal Processing*, vol. 8, no. 5, pp. 966981, 2014.

[13] N. Ravindran, N. Jindal, and H. C. Huang, "Beamforming with finite rate feedback for LOS MIMO downlink channels," *in Global Telecommunications Conference*, 2007. GLOBECOM07. IEEE, pp. 42004204, IEEE, 2007.

[14] L. Sanguinetti, A. Kammoun, and M. Debbah, "Asymptotic analysis of multicell massive MIMO over Rician fading channels," *IEEE International Conference on Acoustics, Speech and Signal Processing (ICASSP)*, pp. 35393543, IEEE, 2017.

[15] J. Cao, D. Wang, J. Li, and Q. Sun, "Uplink Spectral Efficiency Analysis of Multi-Cell Multi-User Massive MIMO over Correlated Ricean Channel," *arXiv preprint arXiv:1707.059*, 15, 07 2017.

[16] S. M. Kay, *Fundamentals of statistical signal processing, Volume I: Estimation Theory*. Prentice Hall PTR, 1993.

ISBN 978-90-827970-1-5 © EURASIP 2018